Long-term changes in summer temperature anomaly patterns in Japan since the early 20th century

Reprinted from *Int. J. Climatol.*, 2014.

INTERNATIONAL JOURNAL OF CLIMATOLOGY
Int. J. Climatol. (2014)
Published online in Wiley Online Library
(wileyonlinelibrary.com) DOI: 10.1002/joc.4241

RMetS
Royal Meteorological Society

Long-term changes in summer temperature anomaly patterns in Japan since the early 20th century

Junpei Hirano[a]* and Takehiko Mikami[b]

[a] *National Research Institute for Earth Science and Disaster Prevention, Ibaraki, Japan*
[b] *Faculty of Liberal Arts, Teikyo University, Hachioji, Japan*

ABSTRACT: The relationship between long-term variations in summer temperature in Japan since the early 20th century and the large-scale atmospheric circulation field was analysed. The combined influence of various circulation predictors on temperature variations was analysed via a multicomponent canonical correlation analysis (CCA). The positive phase of the first CCA mode is related to a positive temperature anomaly across Japan, characterized by a weak blocking high over the Okhotsk Sea, and a strong North Pacific subtropical high (NPSH) over Japan. The positive phase of the second CCA mode corresponds to a positive temperature anomaly in southwestern Japan, and a negative anomaly in northern Japan, characterized by an anticyclonic circulation anomaly over eastern China and a cyclonic anomaly over the northwestern Pacific. By investigating the temporal changes in CCA scores, we detected an abrupt increase in the first CCA score in the early 1910s and a long-term increasing trend in the second CCA score since the early 20th century. The abrupt increase in the first CCA score indicates an abrupt increase in temperature throughout Japan. By investigating changes in the circulation field associated with this abrupt warming, we determined that intensification of zonal flow over the Okhotsk Sea was responsible. The increasing trend of the second CCA score indicates an increase in the regional difference in summer temperatures between northern and southwestern Japan. After investigating changes in the circulation field before and after the mid-20th century, we suggest that the southwestward shift of the NPSH and the weakening of anticyclonic circulation anomalies over the northwestern Pacific were responsible for this increase in the regional temperature difference.

KEY WORDS long-term variations; summer; temperature; Japan; circulation field; canonical correlation analysis

Received 20 February 2013; Revised 21 October 2014; Accepted 28 November 2014

1. Introduction

Summer temperature variations in Japan are characterized by large spatial variability, and notable temperature differences are often observed between northern and southwestern Japan. 'North cool/south hot (north hot/south cool)' temperature anomaly patterns are characterized by negative (positive) temperature anomalies in northern Japan and positive (negative) anomalies in southwestern Japan.

A regional difference is also observed in the long-term temperature trend. Figure 1 shows the spatial distribution of the long-term trend in mean summer (June–August) temperature from 1901 to 2010. In southwestern Japan, a trend of significant warming over the 110-year period is observed. In contrast, significant warming is not observed in northern Japan. As a result, the regional difference in temperature between northern and southwestern Japan has increased over the past century. According to the Japan Meteorological Agency (JMA), this remarkable regional difference in the long-term temperature trend is observed only in summer (JMA, 2005), making these regional differences a unique feature of summer temperature variations in Japan. Investigating the possible causes of these regional differences in the summer temperature trend is important in detecting the mechanism and forcing of summer weather variations in Japan.

Rice crops in northern Japan are frequently damaged owing to anomalously low temperatures during the summer. According to Kondo (1985), severe famines due to cool weather frequently occurred in northern Japan during the early 20th century. Consequently, investigating the regional differences and mechanisms of centennial timescale variations in summer temperature is also crucial in understanding the relationship between climate variations and weather-related disasters, such as cold weather damage.

Detailed mechanisms and characteristics for the summer temperature variability in Japan have primarily been investigated for the latter half of the 20th century. Mikami (1975) presented the summer temperature anomaly patterns in Japan between 1901 and 1974, using principal component analysis (PCA), and investigated the relationship between principal component scores and the 500 mb height fields over the Northern Hemisphere between 1946 and 1970. He showed that the predominant summer temperature anomaly pattern in Japan changed from negative to positive after the early 1910s. He also indicated that

* Correspondence to: J. Hirano, National Research Institute for Earth Science and Disaster Prevention, 3-1 Tennodai, Tsukuba, Ibaraki 305-0006, Japan. E-mail: jhirano06@gmail.com

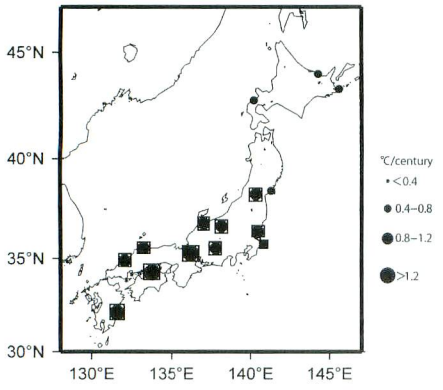

Figure 1. Spatial distribution of the long-term trend in mean summer temperature from 1901 to 2010. Squares indicate the stations with a significant ($p < 0.05$) increasing trend detected by the Mann–Kendall rank statistic.

the occurrence frequency of 'north cool/south hot' temperature anomaly patterns was high from the mid-1950s to the 1970s. However, it is not clear whether this frequent occurrence was related to regional differences in the long-term summer temperature trend (Figure 1). In addition, although Mikami (1975) analysed temperature variations between 1901 and 1974, he could not clarify the relationship between temperature changes and circulation before 1946 owing to a lack of atmospheric circulation data.

Ninomiya and Mizuno (1985) applied an unrotated empirical orthogonal function (EOF) analysis of summer temperature data from 1951 to 1976. However, they also did not analyse the relationship between circulation changes and temperature variations in the early 20th century.

Nishimori (1999) investigated the occurrence of hot and cool summers in Japan, and their relationship to ocean–atmosphere coupled dynamics. He indicated that two types of circulation patterns were related to the occurrence of hot summers since the late 1970s. The first is local anticyclonic circulation in the western Pacific near Japan formed by high sea surface temperatures (SSTs), and the second is caused by the strength of the northwestern part of the North Pacific subtropical high (NPSH).

Yasunaka and Hanawa (2006) investigated the dominant modes of summer temperatures and their inter-annual variations in Japan from 1951 to 2002, using a rotated principal component analysis (RPCA), and investigated the statistical relationships between these modes and atmospheric circulation. They extracted two dominant modes of surface air temperature variations. The first mode represents temperature variations in central regions of Japan that are linked to the strength of the Tibetan high. The second mode represents temperature variations in northern Japan that are associated with the strength of the Okhotsk high.

Fujibe (2004) indicated that extremely high temperatures in major urban areas of Japan can be attributed to the slowly intensifying urban heat island effect and a rapid increase in background warming since the late 1970s. However, the detailed mechanisms of background warming were not clarified.

Many studies have investigated the detailed mechanisms behind variations in the circulation pattern over East Asia, which is closely related to summer temperature variability in northern Japan. Tachibana *et al.* (2004) detected two different anomaly types in the Okhotsk blocking high: the Siberian pattern and the North Pacific pattern. The former has a deep vertical structure, while the latter has a shallow structure, which is closely associated with the cold anomaly of northern Japan. Sato and Takahashi (2007) identified an upper-level pressure anomaly pattern corresponding to the inter-annual variability of the Okhotsk high in midsummer. They indicated that a negative summer temperature anomaly in northern Japan occurred because of advection of the climatological temperature gradient from anomalous wind associated with an upper-level anticyclonic anomaly.

Although these studies investigated summer temperature variations in Japan, and their relationship to large-scale circulation fields for the latter half of the 20th century, studies that focus on the mechanisms behind regional differences in summer temperature trends since the early 20th century are rare (Figure 1). This is primarily due to the lack of atmospheric circulation data for the early 20th century.

Recently, Nagata and Mikami (2010, 2012) used surface pressure data to investigate variations in the western boundaries of the NPSH over East Asia since the early 20th century. According to their results, the western boundary of the NPSH has extended southwestward during the last 100 years, and this extension became more pronounced after the 1950s. Their results suggest that the summer circulation pattern over East Asia changed dramatically after the 1950s. Lo and Hsu (2008) also suggested that the southwestward expansion of the subtropical high ridge from Taiwan to southern China occurred after the early 1950s. However, the relationship between these circulation changes and long-term summer temperature variations in Japan has not been well addressed. In order to clarify these issues, it is necessary to investigate changes in predominant temperature anomaly patterns and their association with circulation patterns using long-term temperature and circulation data from the early 20th century to the present. Until recently, it was difficult to clarify this relationship in detail owing to the lack of reliable atmospheric circulation data before the mid-20th century. Recently, a 20th century reanalysis data set of global atmospheric circulations since 1871 was developed (Compo *et al.*, 2011), allowing a detailed investigation of the relationship between summer temperature variations and large-scale circulation patterns from the early 20th century to the present.

In this study, we attempted to determine the characteristics and mechanism of inter-decadal and long-term changes in predominant summer temperature anomaly patterns in Japan over a 110-year period, using 20th century reanalysis data. In Sections 2 and 3, we describe the data and methods used in this study. In Section 4, we

investigate the relationship between temperature and atmospheric circulation field variations using multicomponent canonical correlation analysis (CCA). We then discuss the changes in circulation fields associated with inter-decadal and long-term changes of the canonical scores. A discussion of the results is addressed in Section 5, and conclusions are presented in Section 6.

2. Data

In order to investigate the relationships between long-term temperature variations and large-scale atmospheric circulations, it is necessary to use long-term continuous temperature data that are not highly influenced by urban-induced warming. Numerous studies indicate that temperature trends, as observed by meteorological stations in Japan, are affected by urbanization (Kato, 1996; Fujibe, 1995, 2009a, 2009b, 2011). The JMA has selected 17 stations to monitor the long-term temperature variations in Japan. According to the JMA, these stations are not strongly influenced by urbanization (JMA, 2012). Das *et al.* (2011) concluded that temperature data provided by these stations were relatively free from urban contamination based on a comparison of SST and the Coupled Model Intercomparison Project Phase 3 (CMIP3) multi-model ensemble results. However, evidence of urban-induced warming has been observed at some of these stations (Fujibe, 2009a, 2011, 2012). Although it is difficult to obtain long-term temperature data that are completely free from urban biases, we believe that using temperature data of these stations is the best way for analysing summer temperature variations, since the heat island effect in urban Japan is more enhanced in winter than in summer (Fujibe, 2011). Among the 17 JMA stations, 15 stations were selected for the current study, since they are located across the four major islands of Japan (Figure 2). Monthly mean temperature data for June, July and August between 1901 and 2010 were used. In this study, summer is defined as June–August, and the seasonal mean temperature for these months was calculated based on monthly temperature data.

In order to investigate the relationship between temperature variability and atmospheric circulation patterns, the 20th Century Reanalysis V2 (20CRv2) data set (Compo *et al.*, 2011) was used. The 20CRv2 data set is a global atmospheric reanalysis data set from 1871 to the present, assimilating only surface pressure reports and using observed SST and sea ice distributions as boundary conditions. An intercomparison with independent radiosonde data indicates that reanalysis data are generally of high quality (Compo *et al.*, 2011). Using the 20CRv2 data set, inter-decadal variability (over 100 years) of the Asian–Pacific Oscillation (APO) (Zhao *et al.*, 2011) and the Hadley circulation (Liu *et al.*, 2012) was successfully revealed.

Although the 20CRv2 data set was developed by assimilating only surface pressure data, upper-level geopotential heights in the Northern Hemisphere are highly correlated with those from radiosondes and other reanalysis data sets (Compo *et al.*, 2011). For example, the 300 hPa level geopotential height from 20CRv2 data around Japan is strongly correlated (≥0.70) with that from other reanalyses (e.g. the ERA 40 reanalysis) and radiosonde data (Compo *et al.*, 2011). We, therefore, considered the 20CRv2 data set reliable enough to represent variations in circulation in our study area.

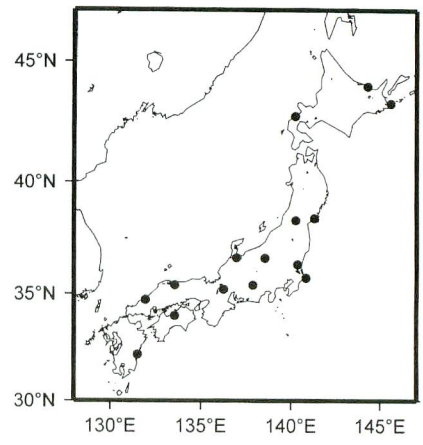

Figure 2. Locations of the 15 meteorological stations used in this study (indicated by black circles).

In this study, monthly mean values of geopotential height data at 1000 and 500 hPa and sea level pressure (SLP) data for East Asia and the western Pacific (100°E–190°E, 0°N–80°N; horizontal resolution is 2° × 2°) were used for 1901–2010. The grid point data of this reanalysis data set were normalized and then weighted by multiplication with the square root of the cosine of latitude, in order to account for the latitudinal variation of the grid area (North *et al.*, 1982).

3. Methods

In the majority of previous studies on temperature variations in Japan, the influence of circulation was analysed based on composite analysis or correlation analysis for each circulation parameter (Mikami, 1975; Ninomiya and Mizuno, 1985; Nishimori, 1999; Tachibana *et al.*, 2004). However, for the combined influence of several different circulation parameters on temperature variability, these methods are insufficient. In contrast, the multicomponent CCA can evaluate the influence of multiple atmospheric circulation parameters on local temperature variability. It is obvious that summer temperature variability in Japan cannot be explained by a single atmospheric circulation parameter. Therefore, we consider the multicomponent CCA an effective way of investigating the combined influence of several different circulation parameters on surface temperature variability.

CCA is a multivariate statistical technique that can investigate the relationships between a set of predictor variables and a set of predictand variables (Hotelling, 1936; Barnett and Preisendorfer, 1987; Zorita *et al.*, 1992;

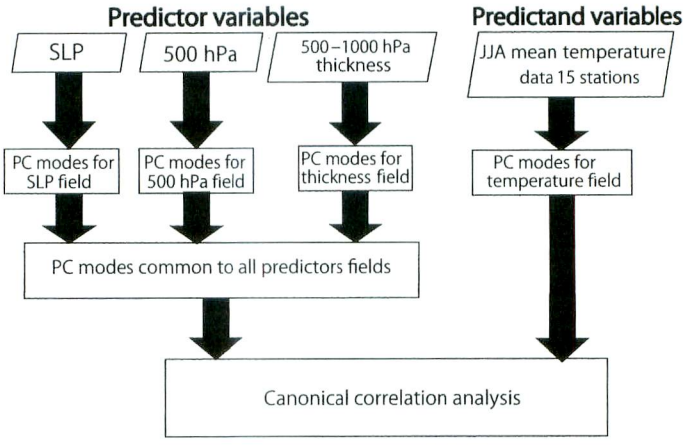

Figure 3. Methodology of the multicomponent CCA used in this study.

Wilks, 1995; von Storch and Zwiers, 1999; Xoplaki *et al.*, 2003a, 2003b, 2004). According to Xoplaki *et al.* (2003a), the CCA selects pairs of spatial patterns for two space- or time-dependent variable sets, such that the time-dependent pattern amplitudes are optimally correlated. CCA is frequently used to investigate the relationship between large-scale circulation patterns and regional climate variations (Zorita *et al.*, 1992; Xoplaki *et al.*, 2003a, 2003b, 2004).

Prior to CCA, the PCA was often used (Barnett and Preisendorfer, 1987; Chen and Chen, 2003; Xoplaki *et al.*, 2003a, 2003b, 2004). The PCA consists of pre-filtering procedures that can reduce the noise of original fields by discarding high-index principal components (Xoplaki *et al.*, 2003a). Applying PCA can also reduce the dimensions of original data. Moreover, PCA can extract independent (orthogonal functions) variables, which can be used as input variables for CCA, from original fields.

To clarify the influence of various circulation predictors of summer temperature variability in Japan, a multicomponent CCA was applied, using a method similar to the method presented by Xoplaki *et al.* (2003a, 2003b, 2004). Using the multicomponent CCA, it is possible to investigate the combined influence of several different circulation predictors on the local temperature variability, as carried out by Xoplaki *et al.* (2003a) over the Mediterranean basin.

In order to perform the multicomponent CCA, the 500 hPa level geopotential height, SLP and 500–1000 hPa layer thickness data were selected as predictor variables. The 500 hPa geopotential height field is used as a predictor variable since several previous studies suggested that it is highly correlated with summer temperature variations in Japan (Mikami, 1975; Nishimori, 1999). In contrast, anomalously cold weather in northern Japan is often caused by a shallow blocking high over the Okhotsk Sea (Tachibana *et al.*, 2004), which is more prominent in the lower troposphere than in the upper or middle troposphere. Consequently, investigating surface pressure systems as well as 500 hPa heights is important to detect the possible mechanisms for summer temperature variations in Japan. Therefore, SLP data are also used as predictors in the CCA. Tachibana *et al.* (2004) also suggested that variations in thickness patterns in the lower troposphere play an important role in forming blocking high over the Okhotsk Sea. Therefore, 500–1000 hPa layer thickness data were used as predictors.

Figure 3 shows the analysis procedures for the multicomponent CCA. Prior to the analysis, predictand and predictor data were normalized, and then an RPCA was applied to both predictor and predictand data to obtain input variables for the CCA.

Two steps of RPCA analysis were applied to predictor variables. (1) In the first step, RPCA was applied to each predictor variable to obtain the dominant PC modes for each predictor data set. As a result, dominant PC modes for the 500 hPa level geopotential height, 500–1000 hPa layer thickness and SLP were obtained (this step is termed 'PC modes-step1'). (2) In the second step, RPCA was applied to scores from PC modes-step1 to obtain the dominant PC modes (this step is termed 'PC modes-step2') that are common to all predictor data sets. At each step, the leading PC modes, which explain more than 80% of the total variance of the original fields, were obtained. (3) Finally, a CCA was applied to calculate linear combinations between the resulting predictor PC modes (from PC modes-step2) and predictand PC modes (from temperature data), so that their corresponding pattern coefficients were optimized and correlated. Then, the CCA provided pairs of canonical patterns and the corresponding time series of canonical scores, in decreasing order of canonical correlation coefficients.

4. Results

4.1. Canonical correlation analysis

Table 1 shows the results of the CCA. In order to confirm the advantages of using a multicomponent CCA, these

Table 1. Results of the CCA.

Predictors	Predictor PCs	Predictand PCs	rCCA1	rCCA2	E
500 hPa	9	4	0.73	0.52	28.9
SLP	12	4	0.75	0.57	41.3
Thickness	9	4	0.71	0.66	38.6
Multicomponent	13	4	0.79	0.72	49.9

Column 1: predictor variables used for CCA. Columns 2 and 3: number predictor and predictand PCs. Columns 4 and 5: canonical correlations for the first two CCA modes. Column 6: total explained variance of temperature by the first two CCA modes. Unit is %.

results were compared to those from a single component CCA. In the multicomponent CCA, calculations were conducted using combined information from multicomponent predictors, including 500 hPa geopotential height, SLP and 500–1000 hPa thickness data. In contrast, for the single component CCA, canonical correlations were calculated using information from each of the single predictor data sets.

Compared to the single component CCA, the explained variance improved using the multicomponent CCA. The results of the CCA indicate that combined multicomponent predictors explained 49.9% of summer temperature variations in Japan, which is higher than those explained by the single component predictor. These results indicate that the combined information from three different circulation predictors can be used to explain the summer temperature variations better than a single circulation predictor. Therefore, it is reasonable to investigate the mechanism of long-term summer temperature variations using the multicomponent CCA. Only a few studies have attempted to explain variations in summer temperature in Japan using combined information on different circulation parameters. Therefore, our results, obtained using multicomponent CCA, are the first of their kind.

The first CCA mode shares 7.4% of the multicomponent predictor variance and 69.3% of the summer temperature variability in Japan. The canonical correlation between the temperature and the multicomponent field coefficient time series is 0.79. The second CCA mode shares 10.5% of the combined predictor variance and 13.6% of the summer temperature variability in Japan. The canonical correlation coefficient is 0.72. The canonical correlation coefficients for the other CCA modes are lower than 0.50. Therefore, we focused on the first and the second CCA modes, omitting other CCA modes.

To monitor the performance of the CCA model, cross validation was generally applied (Barnett and Preisendorfer, 1987; Michaelsen, 1987; Wilks, 1995; von Storch and Zwiers, 1999; Xoplaki *et al.*, 2003a, 2003b, 2004). In the cross-validation process, the CCA model was constructed using all data except for one sample. The excluded data were then predicted using the CCA model (Michaelsen, 1987; Wilks, 1995; von Storch and Zwiers, 1999; Xoplaki *et al.*, 2003a, 2003b, 2004). However, long-term trends in predictand or predictor variables may overestimate the skill of cross validation (Shabbar and Kharin, 2007). In this study, a significant warming trend in temperature is observed in western Japan. Therefore, we consider that the validity of applying cross validation in this study is uncertain. In this study, we divided the 110 years of the study period into calibration and validation periods. The calibration period runs from 1901 to 1955 and the validation period from 1956 to 2010. The CCA model was built up using the calibration period data and the validation period data were then predicted using this CCA model.

The skill of the CCA model was measured via its Brier and correlation scores. The Brier score is defined as $\beta = 1 - (S^2_{FP}/S^2_P)$, where S^2_{FP} is the error variance of the forecasts for the reference predicted variable and S^2_P represents the variance of the predicted variable. If $0 < \beta \leqq 1$, the CCA model is considered successful, whereas $\beta \leqq 0$ indicates that the model produces incorrect results. The correlation score (ρ) is the correlation coefficient between predictions and observations. To reveal the performance of the multicomponent CCA, the spatially averaged values of the Brier (β) and correlation (ρ) scores for all the 15 JMA stations were calculated for the validation period. Area-averaged values of β and ρ are 0.29 and 0.53, respectively. Since the Brier score (β) is higher than 0, we consider that the performance of the multicomponent CCA model was satisfactory.

4.2. Map of canonical spatial patterns

Canonical spatial patterns for the first two leading CCA modes were obtained through regressions between time series of canonical scores and each original field. These canonical spatial patterns can be interpreted as anomalies of each field, associated with the positive phase of each CCA mode.

4.2.1. Canonical spatial patterns of the first CCA mode

The first canonical spatial pattern of the temperature field is characterized by positive temperature anomalies throughout Japan (Figure 4(a)). Positive anomalies are more prominent in northern Japan than in southwestern Japan. This pattern is roughly similar to the first eigenvector patterns obtained by unrotated PCA (Mikami, 1975; Ninomiya and Mizuno, 1985). However, the positive anomalies in northern Japan are more prominent than those obtained from the unrotated PCA.

To determine the robustness of the CCA analysis, we made composite maps for high (and low) score years for the first CCA. When the first CCA score is higher than $+1\sigma$ (or lower than -1σ), the years are selected as high (or low) score years. Composite maps for high (low) score years for the first CCA score are characterized by a positive (negative) temperature anomaly across Japan (Figure 5(a) and (b)). Therefore, we consider that the first CCA mode realistically represents temperature variation patterns.

The first canonical spatial patterns of the 500 hPa geopotential heights (Figure 4(b)) and the SLP field (Figure 4(c)) are characterized by positive anomalies around northern Japan and negative anomalies around the Okhotsk Sea. The positive anomalies seem to represent a northward

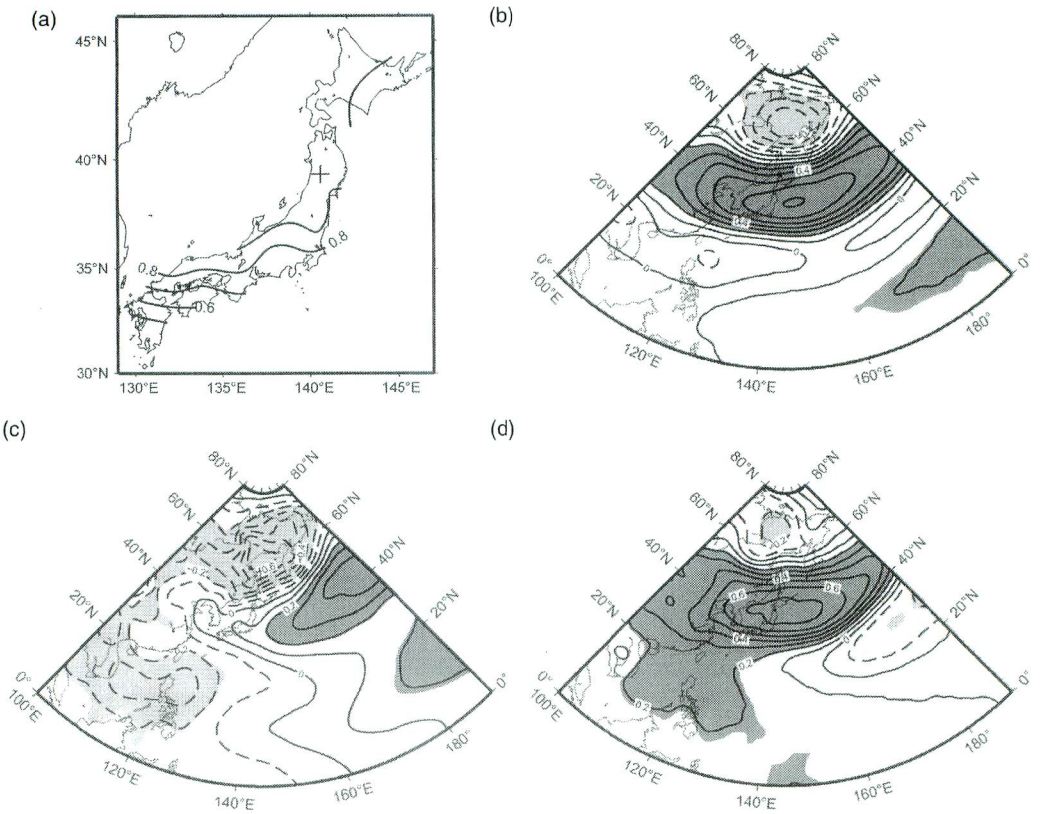

Figure 4. Canonical spatial patterns of the first CCA: (a) temperature patterns (°C), (b) 500 hPa geopotential height patterns (gpm), (c) SLP patterns (hPa) and (d) thickness patterns (gpm). Solid contours indicate positive anomalies. Broken contours indicate negative anomalies. The black (grey) shaded areas indicate that the positive (negative) correlation coefficient exceeded a statistical significance of 5%.

extension of the NPSH. The negative anomalies appear to be related to weakening of the stationary blocking high (the Okhotsk high). The negative anomaly over the Okhotsk Sea is more distinct in the SLP field than in the 500 hPa geopotential heights, which suggests that the blocking high has a shallow vertical structure (Tachibana *et al.*, 2004).

According to Sato and Takahashi (2007), the intensity of the Okhotsk high is only related to temperature variations in northern Japan. Therefore, prominent warm anomalies in northern Japan (Figure 4(a)) and negative SLP anomalies over the Okhotsk Sea (Figure 4(c)) seem to imply a strong relationship between the Okhotsk high and temperatures in northern Japan. It is difficult to identify such coupled circulation-temperature patterns by applying unrotated PCA for only temperature data. Therefore, the use of different methodologies can explain why positive anomalies in northern Japan are more prominent than those obtained using the unrotated PCA (Mikami, 1975; Ninomiya and Mizuno, 1985).

Strong anticyclonic anomalies over Japan (Figure 4(b) and (c)), on the other hand, imply that a strong NPSH brings warm weather throughout Japan. Therefore, higher than normal temperature anomalies throughout Japan (Figure 4(a)) can be explained by a strong NPSH as well as by a weak Okhotsk high.

A positive anomaly over northern Japan can also be observed in the thickness field (Figure 4(d)), and it seems to be associated with a strong NPSH. During these conditions, a strong meridional thickness gradient over the Okhotsk Sea causes zonal flow to strengthen, which prevents the development of a blocking high over the Okhotsk Sea (Tachibana *et al.*, 2004). Therefore, it is reasonable to conclude that the first CCA mode is related to the intensity of zonal flow over the Okhotsk Sea.

4.2.2. *Canonical spatial patterns of the second CCA mode*

The positive phase of the second CCA mode is associated with the occurrence of a 'north cool/south hot' temperature anomaly pattern (Figure 6(a)). Since this pattern is similar to the domain shape dependence pattern of the unrotated PCA (Richman, 1986), we confirm whether this pattern is physically interpretable. We selected high (and low) score years for the second CCA by the method described above for the first CCA. We then created composite maps of temperature anomaly patterns for high and low score years.

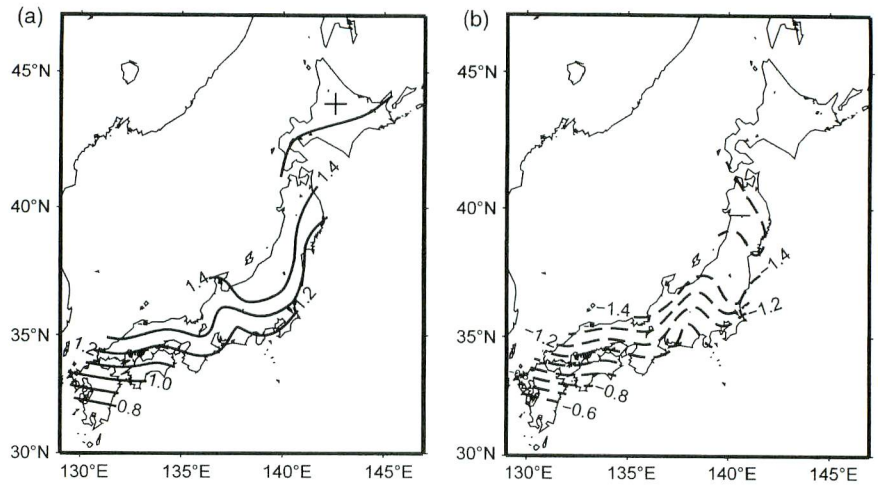

Figure 5. Composite maps of temperature anomaly patterns: (a) high score years of the first CCA and (b) low score years of the first CCA. Unit is °C. Solid contours indicate positive anomalies. Broken contours indicate negative anomalies.

Composite maps of high (low) score years of the second CCA mode actually correspond to the 'north cool/south hot (north hot/south cool)' temperature types (Figure 7(a) and (b)). Therefore, we consider that the second CCA mode realistically represents regional differences in temperature variations in our study area.

The canonical spatial patterns of the 500 hPa geopotential heights and the SLP field (Figure 6(b) and (c)) are characterized by anticyclonic anomalies from eastern China to the Pacific Ocean and cyclonic anomalies over the northern Pacific Ocean near northern Japan. Strong anticyclonic circulation around eastern China brings anomalous warm air towards southwestern Japan. In contrast, anomalous cyclonic circulations over the northern Pacific Ocean are expected to cause a decrease in temperatures in northern Japan. Consequently, enhancement of anticyclonic circulation around eastern China and a cyclonic circulation near northern Japan can cause the occurrence of the 'north cool/south hot' temperature anomaly pattern in Japan.

A strong thickness gradient can be observed over central Japan (Figure 6(d)). This thickness gradient represents the northern boundary of the warm air mass over East Asia, which also plays an important role in the formation of 'north cool/south hot' temperature anomaly patterns.

4.3. Association of the CCA and teleconnection patterns

Since summertime atmospheric circulation systems around Japan are strongly regulated by the intensity of the Asian jet in the upper troposphere and tropical convective activity, we investigate the relationship between the CCA modes and several teleconnection patterns. Enomoto *et al.* (2003) and Enomoto (2004) indicated that development of a deep ridge around Japan is regulated by Rossby wave propagation along the subtropical jet (the Silk Road pattern). We also investigated the relationship between the CCA and the upper troposphere circulation over the Eurasian continent. In addition, tropical convective activity influences the circulation system around Japan. In particular, extratropical wave-train patterns, associated with anomalous convective activity around the Philippine Sea [the Pacific–Japan (P–J) pattern] (Nitta, 1987; Kosaka and Nakamura 2006, 2010), can influence the intensity of the NPSH and the Okhotsk high. Therefore, we investigated the relationship between the CCA modes and the P–J pattern.

4.3.1. Relationship between the Silk Road pattern and the CCA mode

To clarify the relationship between the Silk Road pattern and the CCA modes, we investigated the correlation between CCA scores and the meridional wind field at 200 hPa (Figure 8(a) and (b)). We chose this parameter based on a study by Enomoto (2004) that investigated the Silk Road pattern based on meridional wind data at 200 hPa. According to Enomoto (2004), upper-level alternate meridional winds over mid-latitudes of the Eurasian continent (30°E–150°E, 40°N) indicate Rossby wave propagation along the subtropical jet (the Silk Road pattern).

Figure 8(a) indicates the correlation pattern between the first CCA score and the meridional wind at 200 hPa. Although positive and negative correlations exist for some areas over East Asia, alternate meridional winds along mid-latitudes (30°E–150°E, 40°N) are unclear. Therefore, we consider that the first CCA is not related to the Silk Road pattern.

In contrast, correlation patterns for the second CCA score (Figure 8(b)) show alternate positive and negative correlation areas in mid-latitudes (along 40°N). Over East Asia, the negative correlation area is located over the northern part of the Sea of Japan, and a positive correlation area exists over the northwestern Pacific, east of Japan.

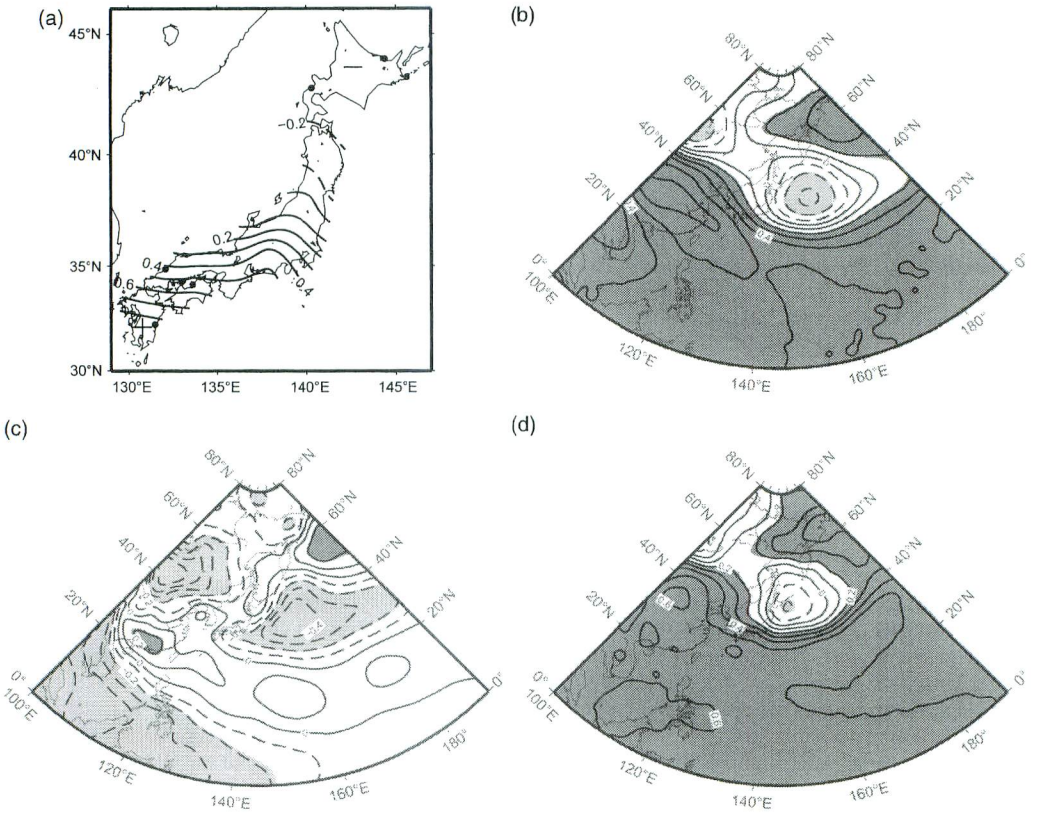

Figure 6. Canonical spatial patterns of the second CCA: (a) temperature patterns (°C), (b) 500 hPa geopotential height patterns (gpm), (c) SLP patterns (hPa) and (d) thickness patterns (gpm). Solid contours indicate positive anomalies. Broken contours indicate negative anomalies. The black (grey) shaded areas indicate that the positive (negative) correlation coefficient exceeded a statistical significance of 5%. The black circles in (a) indicate the stations used to obtain temperature difference between northern and southwestern Japan (see text).

This pattern seems to be a reversal of the Silk Road pattern (Enomoto *et al.*, 2003; Enomoto, 2004). Therefore, we consider that the Silk Road pattern corresponds to the negative phase of the second CCA.

Alternate positive and negative correlation areas from eastern China to the northwestern Pacific imply the development of a ridge over eastern China and a trough near northern Japan. The ridge and the trough seem to be connected with the lower tropospheric pressure and the thickness gradient between southwestern Japan and the area near northern Japan (Figure 6(b)–(d)). Therefore, it seems reasonable that the Silk Road pattern is associated with the regional difference in temperature variations in Japan.

4.3.2. Relationship between the P–J pattern and the CCA mode

In order to clarify the relationship between the CCA modes and the P–J pattern (Nitta, 1987; Kosaka and Nakamura, 2006, 2010), we analysed the correlation between time series of the CCA scores and the 850 hPa level geopotential height field. Since Wakabayashi and Kawamura (2004) defined the P–J index based on geopotential height data at 850 hPa, we also used 850 hPa level geopotential height field data. Figure 9(a) indicates the distribution of correlation coefficients between the first CCA score and the geopotential height. The negative correlation around the Philippine Sea implies anomalous convective activity. A positive correlation area over Japan is a signal of the NPSH. A negative correlation over the Okhotsk Sea implies weakening of the Okhotsk high. All of these features are similar to the extratropical wave-train structure of the P–J pattern (Nitta, 1987; Kosaka and Nakamura, 2006, 2010). Therefore, we consider that the positive phase of the first CCA is associated with the P–J pattern.

Wakabayashi and Kawamura (2004) indicated that the P–J index is positively correlated with summer temperatures in northern and eastern Japan. Since the positive phase of the first CCA accompanies a prominent warm anomaly in northern Japan (Figure 4(a)), our results are in accordance with those of Wakabayashi and Kawamura (2004).

According to Figure 9(b), the positive phase of the second CCA mode is related to a southwestward shift of the NPSH and weakening of the anticyclonic circulation

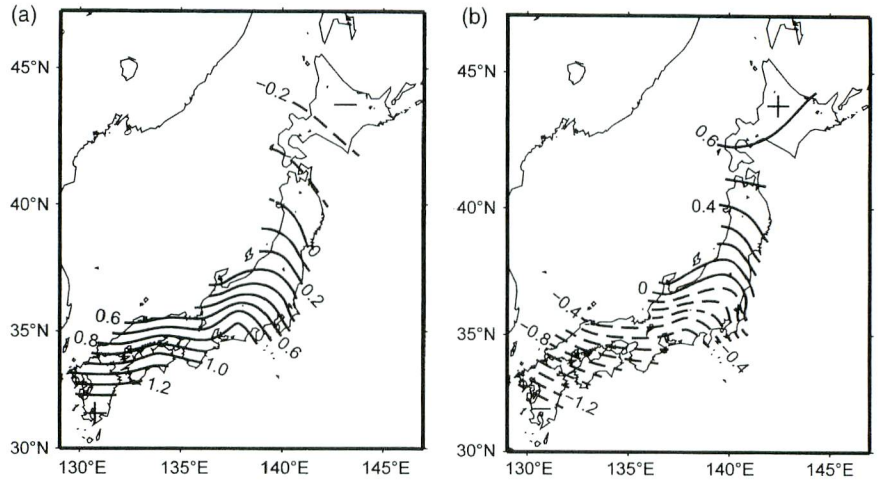

Figure 7. Composite maps of temperature anomaly patterns: (a) high score years of the second CCA and (b) low score years of the second CCA. Unit is °C. Solid contours indicate positive anomalies. Broken contours indicate negative anomalies.

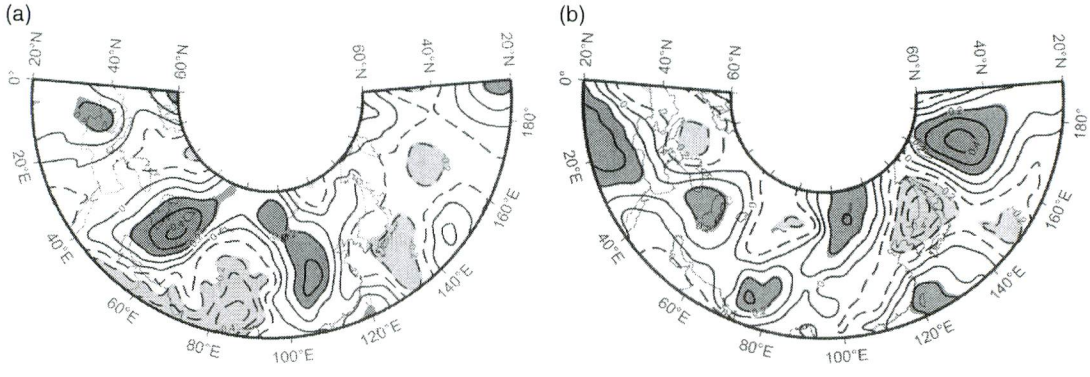

Figure 8. Distribution maps of correlation coefficients between CCA score and 200 hPa level v-wind component: (a) correlation between the first CCA score and (b) correlation between the second CCA score. Solid contours indicate positive correlation. Broken contours indicate negative correlation. The black (grey) shaded areas indicate that the positive (negative) correlation coefficient exceeded a statistical significance of 5%.

over the northern Pacific. However, there are no signs of extratropical wave-train structure. Therefore, we consider that there is no relationship between the second CCA and the P–J pattern.

4.4. Temporal variation of canonical scores

Figure 10(a) and (b) represents the temporal variability of the first and the second CCA scores. First, we tested the time series of CCA scores to determine their correspondence to physical behaviour of summer temperature variability. Since the positive phase of the first CCA mode is associated with positive temperature anomalies throughout Japan (Figure 4(a)), we calculated the correlation coefficient between the time series of the first CCA score and the spatially averaged summer temperature for all of the 15 JMA stations. As a result, we confirmed that the first CCA score is highly correlated with the spatially averaged temperature (correlation coefficient =0.94). With respect to the second CCA score, three JMA stations located in northern and southwestern Japan were selected (see Figure 6(a)). Based on the results shown in Figure 6(a), we calculated the difference in the spatially averaged temperatures of northern and southwestern Japan. The time series of temperature differences between northern and southwestern Japan is highly correlated with variations of the second CCA score (correlation coefficient =0.89). Consequently, we suggest that the leading two CCA modes can explain the physical behaviour of summer temperature variability in Japan over the past 110 years.

4.4.1. Temporal variation of the first CCA score

Temporal variations of the first CCA score (Figure 10(a)) are characterized by an abrupt increase in the scores for the early 1910s. In order to detect statistically the point at which this change occurred, the Lepage test (Lepage, 1971) was applied to the time series of the first CCA

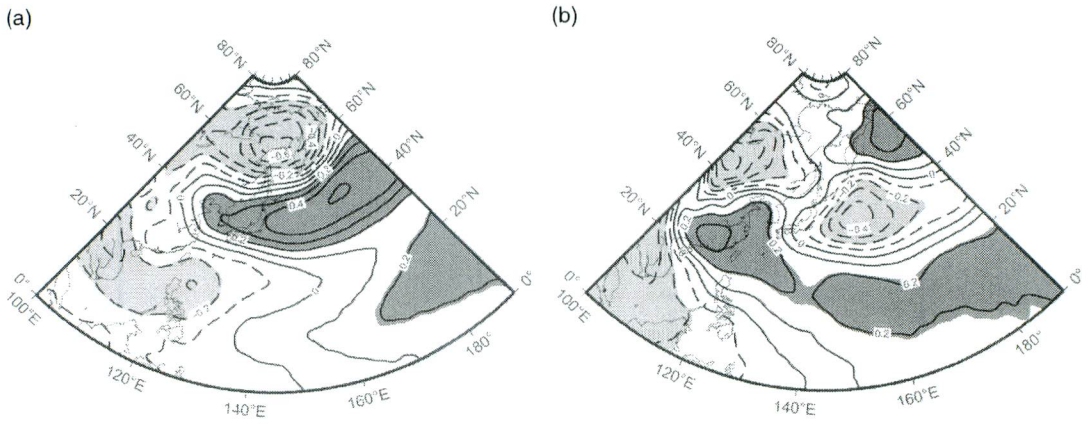

Figure 9. Distribution maps of correlation coefficients between CCA score and 850 hPa level geopotential height: (a) correlation between the first CCA score and (b) correlation between the second CCA score. Solid contours indicate positive correlation. Broken contours indicate negative correlation. The black (grey) shaded areas indicate that the positive (negative) correlation coefficient exceeded a statistical significance of 5%.

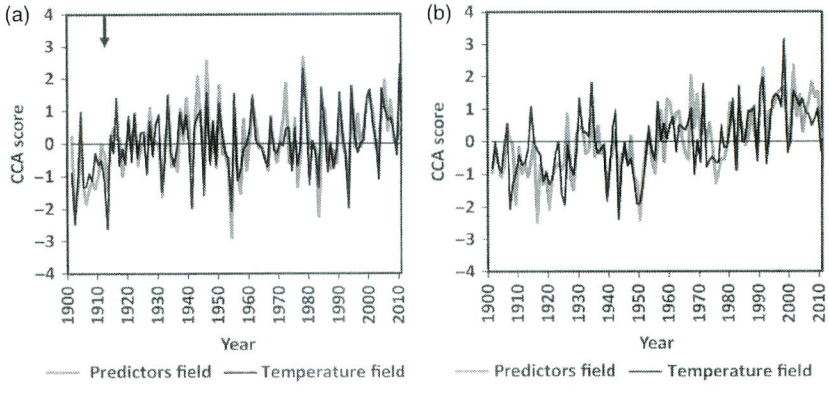

Figure 10. Time series of the canonical scores for (a) the first and (b) the second CCA. The arrow in (a) indicates the abrupt increase in the scores detected by the Lepage test.

score. The Lepage test is a nonparametric test that is used to detect significant differences between two samples. The Lepage test has been often used to detect discontinuous climate changes (Yonetani, 1992, 1993; Inoue and Matsumoto, 2007; Hirano and Matsumoto, 2011). Results of the Lepage test often change depending on the sample sizes (n_1 and n_2). Therefore, we checked the results of this test by changing the sample sizes (n_1 and n_2); we applied the Lepage test three times, changing the sample sizes (n_1 and n_2) from 10 to 12. If more than two tests detect a significant discontinuity ($p < 0.05$) for both temperature and the predictor CCA scores, we recognized that year as the point of abrupt change.

As a result, a significant ($p < 0.05$) abrupt increase in the first CCA score during 1913–1914 was found in both CCA scores of temperature and predictors fields. This indicates an abrupt increase in summer temperature throughout Japan. Prior to this increase, negative scores of the first CCA were predominantly observed, indicating the frequent occurrence of an extremely cool summer throughout Japan before the 1910s. After this increase, the temporal variation of the first CCA score is characterized by large year-to-year variability.

4.4.2. *Temporal variation of the second CCA score*

The temporal variation of the second CCA score (Figure 10(b)) is characterized by a long-term increasing trend. To identify this long-term trend, the Mann–Kendall rank statistic (Kendall, 1938) was applied to the time series of the second CCA score. As a result, a significant ($p < 0.05$) increasing trend was detected in both canonical scores of temperature and predictor fields. This feature indicates an enhancement of the 'north cool/south hot' temperature patterns over the past 110 years. In particular, positive scores are frequently observed after the 1950s. These features are in good accordance with the regional difference in temperature trends shown in Figure 1. This result is also in accordance with the results of Kato (1996), indicating an enhancement of the north–south summer temperature gradient since the 1920s.

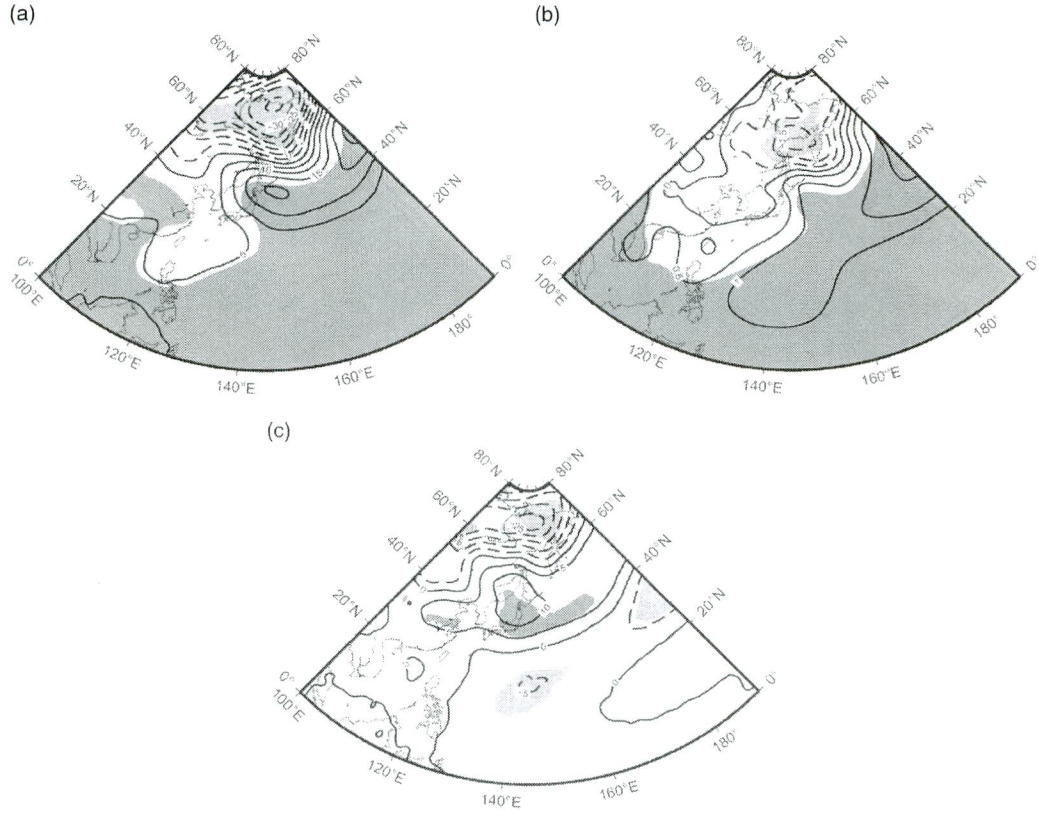

Figure 11. Changes in the (a) 500 hPa geopotential heights (gpm), (b) SLP (hPa) and (c) 500–1000 hPa thickness (gpm) between 1901–1913 and 1914–1926. The black (grey) shaded regions indicate statistically significant increases (decreases); a Student's t-test and $p < 0.05$ were used to indicate significance. Solid contours indicate positive deviations. Broken contours indicate negative deviations.

We also applied the Lepage test to the second CCA score, using the same criteria as for the first CCA. However, we could not detect any abrupt changes in the second CCA score. Therefore, we consider that the increase of the second CCA score is characterized by a linear trend, rather than a discontinuous change.

4.5. Changes in circulation fields associated with inter-decadal variations and long-term trends in canonical scores

In the previous section, the relationship between the circulation patterns and the summer temperature variations over the entire study period was clarified using a CCA. In this section, the mechanisms of inter-decadal changes and long-term trends in canonical scores are discussed by investigating the changes in atmospheric circulation fields associated with changes in canonical scores. First, changes in circulation patterns associated with the abrupt increase in the first CCA score in the early 1910s are described. Additionally, changes in the circulation fields associated with the increasing trend of the second CCA score are discussed.

4.5.1. Changes in circulation fields associated with the abrupt increase of the first CCA score in the early 1910s

In order to determine the mechanism behind the abrupt increase in the first CCA score during 1913–1914, changes in the mean circulation field were investigated for the periods from 1901 to 1913 and 1914 to 1926. Significant ($p < 0.05$) increases in 500 hPa geopotential heights, SLP and thicknesses (Figure 11) can be observed in northern Japan. In contrast, significant decreases in these parameters can be observed around the Okhotsk Sea. These changes lead to an enhancement of the zonal flow over the Okhotsk Sea. As mentioned in Section 4.2, the intensity of the zonal flow over the Okhotsk Sea is related to the first CCA mode. Consequently, we suggest that enhancement of the zonal flow over the Okhotsk Sea was responsible for the abrupt increase in summer temperature throughout Japan in the early 1910s.

4.5.2. Changes in circulation fields associated with the increasing trend of the second CCA score

To determine the possible cause of a long-term increasing trend in the second CCA score (Figure 10(b)), the

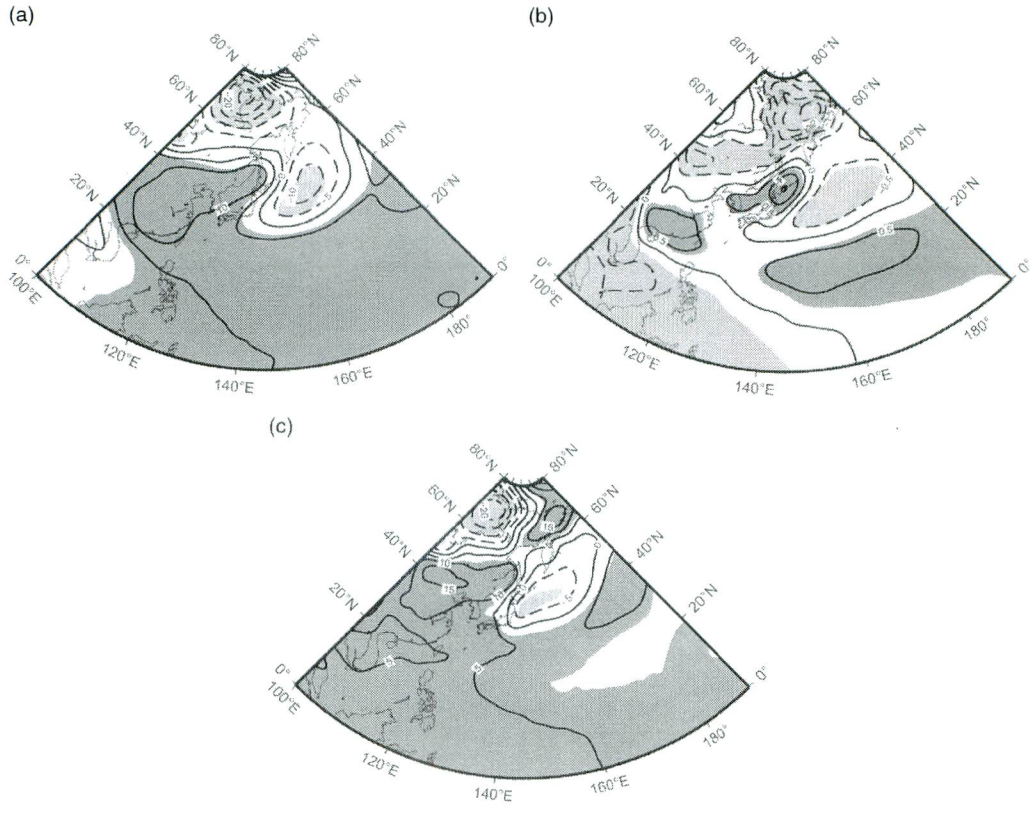

Figure 12. Changes in (a) 500 hPa geopotential heights (gpm), (b) SLP (hPa) and (c) 500–1000 hPa thickness (gpm) between 1901–1950 and 1951–2000. Black (grey) shaded regions indicate statistically significant increases (decreases); a Student's t-test and $p < 0.05$ were used to indicate significance. Solid contours indicate positive deviations. Broken contours indicate negative deviations.

study period was divided into two periods: before 1950 and after 1951. The changes in the mean circulation fields for 1901–1950 and 1951–2000 were then investigated. A distinctive increase in 500 hPa heights, SLP and thicknesses (Figure 12) can be observed from eastern China to the western Pacific Ocean. In contrast, a significant decrease in these parameters can be observed over the North Pacific, near northern Japan. These features indicate a southwestward shift of the NPSH over East Asia, which corresponds to the results of previous studies (Nagata and Mikami, 2010, 2012 ; Lo and Hsu, 2008).

An increase in heights and thicknesses was also observed from eastern China to the Sea of Japan, seemingly related to the development of a ridge over this area. Consequently, we suggest that the frequent occurrence of the 'north cool/south hot' temperature anomaly patterns after the 1950s was caused by the southwestward shift of the NPSH and the development of a ridge over eastern China.

As discussed in Section 4.3, the negative phase of the second CCA is associated with the Silk Road pattern. Therefore, we investigated the changes in the upper tropospheric circulation field before 1950 and after 1951 to understand the relationship between the Silk Road pattern and the temperature changes. Figure 13 indicates changes in the 200 hPa level meridional wind field before 1950 and after 1951. Positive and negative deviation areas alternately appeared in mid-latitudes of the Eurasian continent, which is similar to the meridional wind field pattern associated with the second CCA (Figure 8(b)).

These changes seem to imply weakening of the Silk Road pattern, which accompanies deepening of the ridge over eastern China and the trough near northern Japan. These upper troposphere changes appear connected to the lower tropospheric pressure and the thickness gradient between eastern China and the area near northern Japan (Figure 12). Therefore, we consider that weakening of the Silk Road pattern also contributes to the increase in the second CCA after the mid-20th century.

5. Discussion

In this section, we compare the results of our study to those of previous studies. The frequent occurrence of low temperatures during summers before the early 1910s and the change in the predominant temperature anomaly patterns in the early 1910s compare well with the results of Mikami

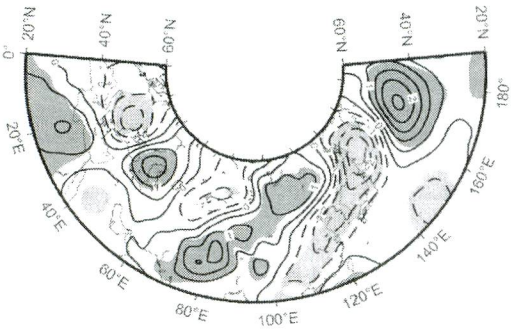

Figure 13. Changes in 200 hPa level v-wind ($m\,s^{-1}$) between 1901–1950 and 1951–2000. Black (grey) shaded regions indicate statistically significant increases (decreases); a Student's t-test and $p < 0.05$ were used to indicate significance. Solid contours indicate positive deviations. Broken contours indicate negative deviations.

(1975). The JMA (2005) also reported that the frequency of 'extreme cool summers' was high in the early 1900s and decreased after the 1910s, which supports our results. Nishimori (1999) indicated that summer temperatures in mainland Japan were low from the late 1890s to the early 1910s and became slightly higher after the mid-1910s, which is also in accordance with our results.

However, the above-mentioned studies did not investigate the cause of an abrupt warming in summer temperatures after the early 1910s. In this study, and for the first time, we discovered that this abrupt increase in temperature is attributable to the strengthening of zonal flow over the Okhotsk Sea. Further studies are needed to clarify the reasons behind this strengthening.

A regional difference in the summer temperature trend (Figure 1) can be explained by an increase in the second CCA score. Mikami (1975) mentioned that a 'north cool/south hot' temperature anomaly pattern frequently appeared between the 1950s and 1970s. Kato (1996) also indicated an increase in the north–south temperature gradient in summer since the 1920s. However, they did not mention the mechanism for this trend. In this study, we determined that the increasing trend of 'north cool/south hot' patterns is related to a southwestward shift of the NPSH and the development of a ridge over eastern China after the 1950s. We revealed that weakening of the Silk Road pattern also contributed to the enhancement of 'north cool/south hot' temperature patterns in Japan.

Since the southwestward shift of the NPSH after the 1950s was only recently investigated in detail, there are few studies on the mechanisms behind this phenomenon. Although several studies investigated a southwestward extension of the NPSH over East Asia from the late 1970s (Gong and Ho, 2002; He and Gong, 2002; Zhou *et al.*, 2009), they did not consider a southwestward extension of the NPSH after the 1950s. Results from Nagata and Mikami (2010, 2012), on the other hand, indicated that a southwestward extension of the NPSH became evident after the 1950s. Lo and Hsu (2008) also suggested that a southwestward expansion of the subtropical high ridge from Taiwan to southern China occurred after the early 1950s. Consequently, further studies are needed to clarify the reasons for this southwestward shift.

Although large-scale atmospheric circulation patterns are highly correlated with summer temperature variations in Japan, several other local-scale factors may also contribute to temperature variations. Fujibe (2004) discovered an increasing trend in summertime daily maximum and minimum temperatures, for an area ranging from central to western Japan, since the 1970s. Although this situation seems to match a recent high occurrence frequency of 'north cool/south hot' temperature anomaly patterns, Fujibe (2004) suggested that the amplitude of this warming is more significant in the boundary layer than in the free atmosphere. Therefore, further studies need to be conducted to clarify the physical process in the boundary layer that caused this recent rapid warming.

Urban-induced warming is detectable not only in densely populated areas but also at sparsely urbanized sites (Fujibe, 2009a, 2009b, 2011, 2012). This can cause a bias in the evaluation of background temperature variations. Therefore, we discuss the influence of urban-induced biases in our analysis. According to Fujibe (2009b), the background (non-urban) warming trend in centennial temperature data is larger in western Japan and smaller in northern Japan. This feature is prominent in summer. This regionality appears similar to the spatial pattern of the second CCA mode (Figure 6(a)). In contrast, there are no remarkable regional differences in urban-induced temperature trends (Fujibe, 2009b). Therefore, we cannot explain the increasing trend in the second CCA by urbanization, and we consider that there is little evidence that an urban-induced bias is included in the second CCA.

The first CCA mode has a unimodal canonical pattern, which accompanies a prominent positive temperature anomaly in northern Japan (Figure 4(a)). This pattern also cannot be explained by an urban bias, as there is no evidence for such a prominent urban bias in northern Japan. Moreover, urban-induced bias would have been more pronounced after the 1960s (Fujibe, 2009b); however, in the first CCA score, no significant trend exists after an abrupt warming in the early 1910s. Based on these facts, we consider that results of this study are influenced by background climatic changes rather than an urban-induced bias. CCA and RPCA act as filtering processes (Xoplaki *et al.*, 2003a, 2003b) to eliminate some temperature components that are not connected to large-scale circulation. Therefore, we consider that the principles behind the methodology explain the absence of an urban warming signal in our results.

6. Conclusions

In this study, we investigated the inter-decadal and long-term changes in predominant summer temperature anomaly patterns in Japan, for the past 110 years, using

a multicomponent CCA. Results of the multicomponent CCA indicate that, since the early 20th century, 49.9% of the summer temperature variations in Japan can be explained by a combination of three large-scale predictor fields. The positive phase of the first CCA mode is related to an above-normal temperature anomaly throughout Japan, which, in turn, is related to the strong zonal flow over the Okhotsk Sea. The positive phase of the second CCA mode corresponds to a positive temperature anomaly in southwestern Japan and a negative anomaly in northern Japan, which is related to the anticyclonic circulation anomaly over eastern China and the cyclonic anomaly over the northwestern Pacific Ocean near the northern coast of Japan. We also revealed that the negative phase of the second CCA corresponds to the Silk Road pattern.

The mechanisms of inter-decadal and long-term changes in predominant temperature anomaly patterns were investigated by examining the changes in circulation patterns associated with the changes in CCA scores. The major results of our study are summarized as follows.

(1) An abrupt increase in the first CCA score was detected for the early 1910s, which indicated an abrupt warming in summer temperature for the entire country of Japan.
(2) By investigating the changes in the circulation pattern associated with this abrupt change, we suggest that this abrupt change is attributed to strengthening of the zonal flow over the Okhotsk Sea.
(3) A long-term increasing trend was discovered, on a centennial timescale, for the occurrence frequency of the 'north cool/south hot' temperature anomaly patterns. This increasing trend became more evident after the 1950s.
(4) We suggest that the increasing trend in the occurrence frequency of the 'north cool/south hot' temperature anomaly patterns is attributable to a southwestward shift of the NPSH and the development of a ridge over eastern China after the mid-20th century.

Acknowledgements

We would like to thank Associate Professor Masumi Zaiki of Seikei University for her valuable comments and suggestions. Some figures were created with the Generic Mapping Tools (GMT) graphic system developed by Wessel and Smith in 1995.

References

Barnett P, Preisendorfer W. 1987. Origins and levels of monthly and seasonal forecast skill for United States air temperature determined by canonical correlation analysis. *Mon. Weather Rev.* **115**: 1825–1850.

Chen D, Chen Y. 2003. Association between winter temperature in China and upper air circulation over East Asia revealed by canonical correlation analysis. *Glob. Planet. Change* **37**: 315–325.

Compo G, Whitaker J, Sardeshmukh P, Matsui N, Allan R, Yin X, Gleason B, Vose R, Rutledge G, Bessemoulin P, Bronnimann S, Brunet M, Crouthamel R, Grant A, Groisman P, Jones P, Kruk M, Kruger A, Marshall G, Maugeri M, Mok H, Nordli Ø, Ross T, Trigo R, Wang X, Woodruff S, Worley S. 2011. The twentieth century reanalysis project. *Q. J. R. Meteorol. Soc.* **137**: 1–28.

Das L, Annan JD, Hargreaves JC, Emori S. 2011. Centennial scale warming over Japan: are the rural stations really rural? *Atmos. Sci. Lett.* **12**: 362–367.

Enomoto T. 2004. Interannual variability of the Bonin High associated with the propagation of Rossby waves along the Asian jet. *J. Meteorol. Soc. Jpn.* **82**: 1019–1034.

Enomoto T, Hoskins BJ, Matsuda Y. 2003. The formation mechanism of the Bonin high in August. *Q. J. R. Meteorol. Soc.* **129**: 157–178.

Fujibe F. 1995. Temperature rising trends at Japanese cities during the last hundred years and their relationships with population, population increasing rates and daily temperature ranges. *Pap. Meteorol. Geophys.* **46**: 35–55.

Fujibe F. 2004. Features of extremely high summertime temperatures in Japan in recent years. *Geogr. Rev. Jpn.* **77**: 119–132 (in Japanese with English abstract).

Fujibe F. 2009a. Detection of urban warming in recent temperature trends in Japan. *Int. J. Climatol.* **29**: 1811–1822.

Fujibe F. 2009b. Evaluation of background and urban warming trends base on centennial temperature data. *Pap. Meteorol. Geophys.* **63**: 43–56.

Fujibe F. 2011. Urban warming in Japanese cities and its relation to climate change monitoring. *Int. J. Climatol.* **31**: 162–173.

Fujibe F. 2012. Dependence of long-term temperature trends on wind and precipitation at urban stations in Japan. *J. Meteorol. Soc. Jpn.* **90**: 525–534.

Gong DY, Ho CH. 2002. Shift in the summer rainfall over the Yangtze River valley in the late 1970s. *Geophys. Res. Lett.* **29**: 78-1–78-4, doi: 10.1029/2001GL014523.

He XZ, Gong DY. 2002. Interdecadal change in western Pacific subtropical high and climatic effects. *J. Geogr. Sci.* **12**: 202–209.

Hirano J, Matsumoto J. 2011. Secular and seasonal variations of winter monsoon weather patterns in Japan since the early 20th century. *Int. J. Climatol.* **31**: 2330–2337.

Hotelling H. 1936. Relations between two sets of variables. *Biometrika* **28**: 321–377.

Inoue T, Matsumoto J. 2007. Abrupt climate changes observed in late August over central Japan between 1983 and 1984. *J. Clim.* **20**: 4957–4967.

JMA. 2005. Unusual weather report 2005 (report on recent climate change 2005 – reviews and outlook for the future). Japan Meteorological Agency, Tokyo (in Japanese).

JMA. 2012. Climate change monitoring report 2012. Japan Meteorological Agency, Tokyo (in Japanese).

Kato H. 1996. A statistical method for separating urban effect trends from observed temperature data and its application to Japanese temperature records. *J. Meteorol. Soc. Jpn.* **74**: 639–653.

Kendall MG. 1938. A new measure of rank correlation. *Biometrika* **30**: 1219–1234.

Kondo J. 1985. A review on a connection among the volcanic eruption, unusual weather, bad crops, and social situation recent three hundred years. *Tenki* **32**: 157–167 (in Japanese).

Kosaka Y, Nakamura H. 2006. Structure and dynamics of the summertime Pacific-Japan (PJ) teleconnection pattern. *Q. J. R. Meteorol. Soc.* **132**: 2009–2030.

Kosaka Y, Nakamura H. 2010. Mechanisms of meridional teleconnection observed between a summer monsoon system and a subtropical anticyclone. Part I: the Pacific-Japan pattern. *J. Clim.* **23**: 5085–5108.

Lepage Y. 1971. A combination of Wilcoxon's and Ansari–Bradley's statistics. *Biometrica* **58**: 213–217.

Liu J, Song M, Hu Y, Ren X. 2012. Changes in the strength and width of the Hadley Circulationsince 1871. *Clim. Past* **8**: 1169–1175.

Lo TT, Hsu HH. 2008. The early 1950s regime shift in temperature in Taiwan and East Asia. *Clim. Dyn.* **31**: 449–461.

Michaelsen J. 1987. Cross-validation in statistical climate forecast models. *J. Appl. Meteorol. Climatol.* **26**: 1589–1600.

Mikami T. 1975. Representation of the anomaly patterns of summer temperature over Japan using principal component analysis and its dynamic climatic considerations. *Geogr. Rev. Jpn.* **48**: 784–797 (in Japanese with English abstract).

Nagata R, Mikami T. 2010. Long-term variability of the North Pacific subtropical high over East Asia and its relation to sea surface temperature in the tropical Pacific. *Ann. Ochanomizu Geogr. Soc.* **50**: 99–105 (in Japanese with English abstract).

Nagata R, Mikami T. 2012. Long-term variability of the western edge of the North Pacific subtropical high and its relation to summer temperature over Japan, 1901–2000. *Geogr. Rev. Jpn.* **85**: 508–516 (in Japanese with English abstract).

Ninomiya K, Mizuno H. 1985. Anomalous cold spell in summer over northeastern Japan caused by northeasterly wind from polar maritime airmass. Part 1. EOF analysis of temperature variation in relation to the large-scale situation causing the cold summer. *J. Meteorol. Soc. Jpn.* **63**: 845–857.

Nishimori M. 1999. Analysis of the characteristics of hot and cool summer in Japan. *Tenki* **46**: 267–280 (in Japanese).

Nitta T. 1987. Convective activities in the tropical western Pacific and their impact on the Northern Hemisphere summer circulation. *J. Meteorol. Soc. Jpn.* **65**: 373–390.

North GR, Moeng FJ, Bell TL, Cahalan RF. 1982. The latitude dependence of the variance of zonally averaged quantities. *Mon. Weather Rev.* **110**: 319–326.

Richman MB. 1986. Rotation of principal components. *J. Climatol.* **6**: 293–335.

Sato N, Takahashi M. 2007. Dynamical processes related to the appearance of the Okhotsk high during early midsummer. *J. Clim.* **20**: 4982–4994.

Shabbar A, Kharin V. 2007. An assessment of cross-validation for estimating skill of empirical seasonal forecasts using a global coupled model simulation. *CLIVAR Exch.* **12**(4): 10–12.

Tachibana Y, Iwamoto T, Ogi M, Watanabe Y. 2004. Abnormal meridional temperature gradient and its relation to the Okhotsk high. *J. Meteorol. Soc. Jpn.* **82**: 1399–1415.

Von Storch H, Zwiers FW. 1999. *Statistical Analysis in Climate Research*. Cambridge University Press: Cambridge, UK.

Wakabayashi S, Kawamura R. 2004. Extraction of major teleconnection patterns possibly associated with anomalous summer climate in Japan. *J. Meteorol. Soc. Jpn.* **82**: 1577–1588.

Wilks DS. 1995. *Statistical Methods in the Atmospheric Sciences*. International Geophysics Series 59, Academic Press: New York, NY.

Xoplaki E, González-Rouco JF, Luterbacher J, Wanner H. 2003a. Mediterranean summer air temperature variability and its connection to the large-scale atmospheric circulation and SSTs. *Clim. Dyn.* **20**: 723–739.

Xoplaki E, González-Rouco JF, Gyalistras D, Luterbacher J, Rickli R, Wanner H. 2003b. Interannual summer air temperature variability over Greece and its connection to the large scale atmospheric circulation and Mediterranean SSTs 1950–1999. *Clim. Dyn.* **20**: 537–554.

Xoplaki E, González-Rouco JF, Luterbacher J, Wanner H. 2004. Wet season Mediterranean precipitation variability: influence of large scale dynamics and predictability. *Clim. Dyn.* **23**: 63–78.

Yasunaka S, Hanawa K. 2006. Interannual summer temperature variations over Japan and their relation to large-scale atmospheric circulation field. *J. Meteorol. Soc. Jpn.* **84**: 641–652.

Yonetani T. 1992. Discontinuous precipitation in Japan after 1900 detected by the Lepage test. *J. Meteorol. Soc. Jpn.* **70**: 95–104.

Yonetani T. 1993. Detection of long-term trend, cyclic variation and step-like change detected by the Lepage test. *J. Meteorol. Soc. Jpn.* **71**: 415–418.

Zhao P, Yang S, Wang H, Zhang Q. 2011. Interdecadal relationships between the Asian–Pacific Oscillation and Summer Climate Anomalies over Asia, North Pacific, and North America during a recent 100 Years. *J. Clim.* **24**: 4793–4799.

Zhou T, Yu R, Zhang J, Drange H, Cassou C, Deser C, Hodson DLR, Sanchez-Gomez E, Li J, Keenlyside N, Xin X, Okumura Y. 2009. Why the Western Pacific Subtropical High has extended westward since the late 1970s. *J. Clim.* **22**: 2199–2215.

Zorita E, Kharin V, von Storch H. 1992. The atmospheric circulation and sea surface temperature in the North Atlantic area in winter: their interaction and relevance for Iberian precipitation. *J. Clim.* **5**: 1097–1108.

Reprinted from *Int. J. Climatol.*, *2014.*